Journal of Innovative Optical Health Sciences
Vol. 6, No. 3 (2013) 1350027 (6 pages)

DOI: 10.1142/S1793545813500272

World Scientific
www.worldscientific.com

A SIMULTANEOUS MULTI-PROBE DETECTION LABEL-FREE OPTICAL-RESOLUTION PHOTOACOUSTIC MICROSCOPY TECHNIQUE BASED ON MICROCAVITY TRANSDUCER

YONGBO WU*, ZHILIE TANG*,†,‡, YAN CHI* and LIRU WU*
*School of Physics and Telecom Engineering, South China Normal University
Guangzhou 510006, P. R. China
†Laboratory of Quantum Information Technology, South China Normal University
IMOT, Guangzhou 510006, P. R. China
‡tangzhl@scnu.edu.cn

Received 27 May 2013
Accepted 26 June 2013
Published 24 July 2013

We demonstrate the feasibility of simultaneous multi-probe detection for an optical-resolution photoacoustic microscopy (OR-PAM) system. OR-PAM has elicited the attention of biomedical imaging researchers because of its optical absorption contrast and high spatial resolution with great imaging depth. OR-PAM allows label-free and noninvasive imaging by maximizing the optical absorption of endogenous biomolecules. However, given the inadequate absorption of some biomolecules, detection sensitivity at the same incident intensity requires improvement. In this study, a modulated continuous wave with power density less than $3\,mW/cm^2$ (1/4 of the ANSI safety limit) excited the weak photoacoustic (PA) signals of biological cells. A microcavity transducer is developed based on the bulk modulus of gas five orders of magnitude lower than that of solid; air pressure variation is inversely proportional to cavity volume at the same temperature increase. Considering that a PA wave expands in various directions, detecting PA signals from different positions and adding them together can increase detection sensitivity and signal-to-noise ratio. Therefore, we employ four detectors to acquire tiny PA signals simultaneously. Experimental results show that the developed OR-PAM system allows the label-free imaging of cells with weak optical absorption.

Keywords: Multi-probe; label-free; optical-resolution photoacoustic microscopy.

1. Introduction

Optical-resolution photoacoustic microscopy (OR-PAM) is an emerging optical−acoustic hybrid technology for micrometer- or submicrometer-scale high-resolution imaging.[1−3] This technology involves the detection of the endogenous optical absorption of

the sample and is critical for important biomedical applications such as the study of cancer cells.[3–6] OR-PAM generally involves the use of a focused laser beam with a microscope objective in photoacoustic (PA) excitation. The lateral resolution of OR-PAM is determined by tight optical focusing capability with a microscope objective.[7,8] Compared with mainstream microscopy technologies such as confocal microscopy, optical coherence tomography and fluorescence microscopy, OR-PAM combines the advantages of rich optical contrast, label-free and noninvasive imaging, and provision of both anatomical and functional information.[9–13] Thus, OR-PAM is a premier microscopic imaging tool in biomedicine.

PAM generally utilizes a short-pulsed laser to generate PA signals to be detected by an acoustic transducer such as a piezoelectric ceramic transducer[14] and a polyvinylidene fluoride needle hydrophone.[15,16] Given the strong attenuation of ultrasound waves in air, acoustic coupling between the sample and the acoustic transducer is required. This requirement is often difficult for PAM of biomedical cell samples, thereby limiting the practical applicability of the technique. We present an OR-PAM system that employs a modulated continuous wave (CW) laser source for excitation and simultaneous multi-probe microscopy acquisition technique to obtain PA signals in air without any coupling agent. Increasing the detection sensitivity of a CW-mode OR-PAM system is the primary challenge because the PA signals induced by CW lasers are too weak, especially when cells with weak optical absorption are involved. Air pressure variation is inversely proportional to cavity volume at the same temperature increase. Considering that PA waves expand in various directions, we adopt simultaneous multi-probe acquisition technique to detect PA signals from different positions and add them together to increase detection sensitivity and signal-to-noise ratio (SNR).

2. Methods

2.1. *Principle of simultaneous multi-probe microscopy acquisition technique*

Based on Rosencwaig–Gersho's theory,[17] a closed microcavity model of a semi-spherical cell with radius R was established (see Fig. 1). The sample is

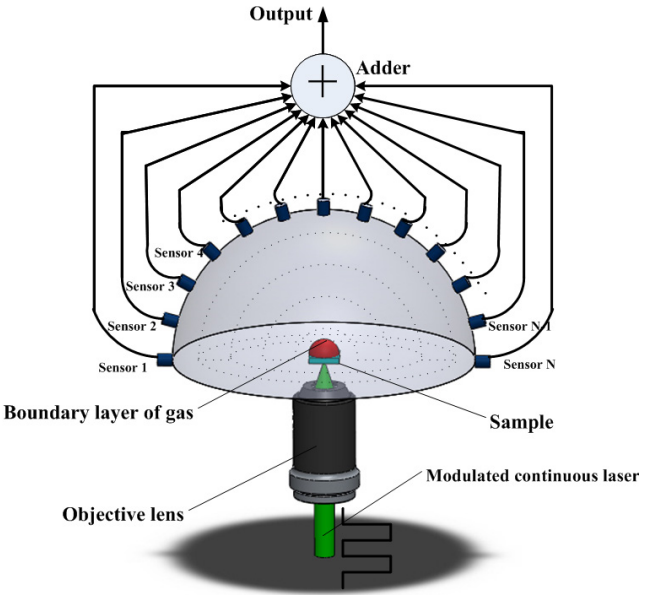

Fig. 1. Principle of simultaneous multi-probe microscopy with a PA transduce.

mounted such that its front surface is exposed to the gas (air) within the cell and its back surface is against an optical window with poor thermal properties. We assume that the gas and optical window do not absorb light. When a chopped monochromatic light source was focused on the sample with an objective lens, an acoustic signal was generated from the periodic heat flow from the sample to the surrounding gas. When the temperature in the gas attenuated rapidly to zero with an increase in the distance from the surface of the sample, a boundary layer (see Fig. 1) whose thickness is $2\pi\mu g$ ($\sim 0.2\,\text{mm}$) was defined. μ_g is the thermal diffusion length. If we assume that the rest of the gas responds to the action of this piston adiabatically, the incremental pressure can be determined by

$$\delta P(t) = \frac{\gamma P_0}{V_0}\delta V = \frac{\gamma P_0}{V_0} \bullet \frac{2\pi\mu_g \bar{\phi}(t)}{T_0} S, \qquad (1)$$

where P_0 and V_0 are ambient pressure and volume, respectively, γ is the ratio of the specific heat and δV is the incremental volume. According to the ideal gas law, δV can estimate the product of the boundary layer's radial displacement by periodic heating $(2\pi\mu_g\bar{\phi}(t)/T_0)$ and the superficial area of boundary (S), where T is the direct current (DC) component of the temperature on the sample surface and $\bar{\phi}(t)$ is the spatially averaged temperature of the gas within the boundary layer (which

depends on the absorption coefficient of the sample and on the illuminated light).

At the same conditions of temperature change, reducing the volume of the cell can effectively increase detection sensitivity. Considering that PA waves expand in various directions, simultaneously detecting PA signals with the same radius from different positions and adding them together can increase detection sensitivity and SNR because the increased sensitivity does not change the volume of the cell (see Fig. 1). The total output of the microcavity PA transducer with N sensors becomes N times the output of one sensor.

2.2. *OR-PAM system*

A schematic of the experimental setup is shown in Fig. 1. A CW laser (Argon ion laser, 35 LAL 515, CVI Melles Griot, USA) with a wavelength of 514.5 nm was utilized as the irradiation source in the system. The CW laser beam modulated by a chopper (SR540, SRS, USA) at 2.5 kHz was scanned with a 2D scanning galvanometer (6231C, Cambridge Technology, USA). A field flattening lens with magnification of 4x (NA = 0.13, UPLFLN4×, Olympus, Japan), 10x (NA = 0.30, UPLFLN10×, Olympus, Japan), 20x (NA = 0.50, UPLFLN20×, Olympus, Japan) and 40x (NA = 0.75, UPLFLN40×, Olympus, Japan) was employed as the objective lens to focus the beam on a tight spot on the sample at an intensity of 3 mW/cm^2, which is lower than the ANSI laser safety standard (12.73 mW/cm^2).[18] The sample was sealed in the multi-probe transducer (red dashed box in Fig. 2), which consisted of a microcavity, two microchannels, two resonant cavities and four microphones. The microcavity had a volume of $\sim$0.8 mm^3. The sample was attached to its opening of optical window. The focused modulated laser caused a spatially and temporally abrupt temperature increase in the focal zone inside the sample and thereby excited the PA waves in the microcavity. The PA waves were immediately transferred to the resonant cavity through the microchannel with a diameter of 0.25 mm and length of 200 mm and simultaneously detected by four microphones (customized with 2.5 kHz central frequency and 10 mv/Pa sensitivity). The PA signals in the four channels were added together with an adder, amplified with a preamplifier (SR550, SRS, USA), and sent to a lock-in amplifier (SR830, SRS, USA) for demodulation and further amplification. The

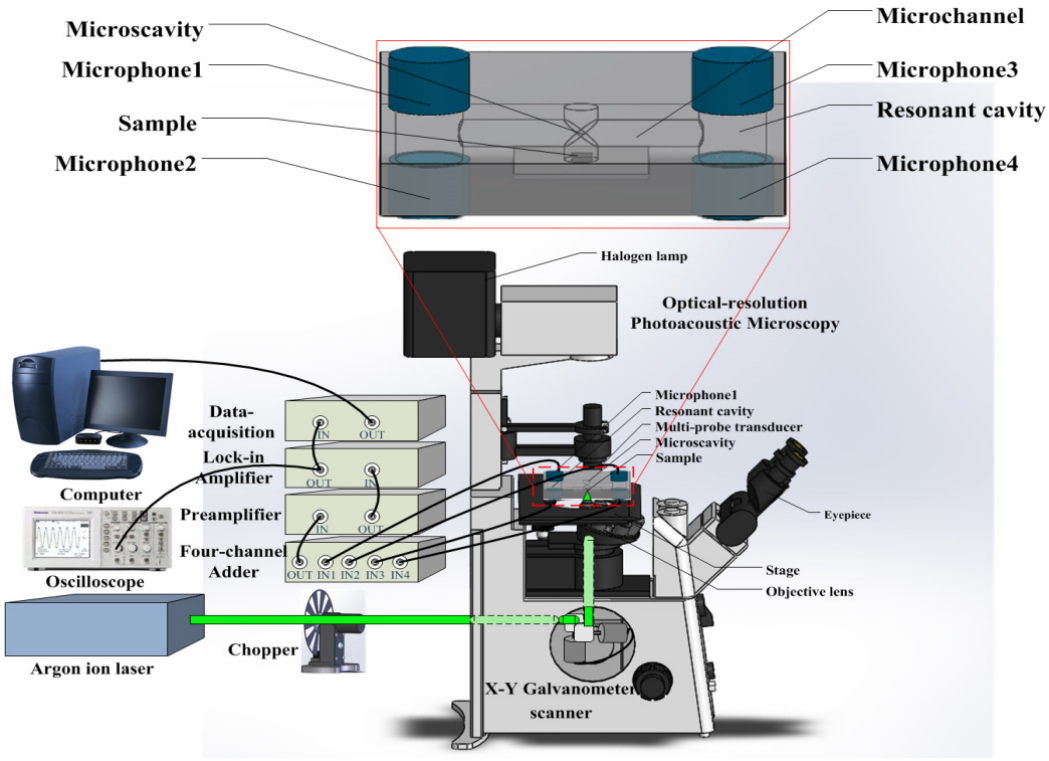

Fig. 2. Schematic of multi-probe detection CW-mode OR-PAM system.

spatial distribution of the amplitude of the PA signals was acquired and stored on the data acquisition board (PCI6115, NI, USA) of a computer.

3. Results and Discussion

3.1. *Lateral resolution of the OR-PAM system*

Lateral resolution can be estimated by the formula $0.51\lambda/\mathrm{NA}$. A resolution test target (JJG 827-1993, RTA-07) was imaged with a 20× objective lens (NA = 0.5) to quantify the lateral resolution of the system. Group 25, which has the highest resolution, was selected for imaging. The width of the bar was 1.25 μm [see Fig. 3(a)]. The PA amplitude values along a line crossing the edge of a bar were fitted by the theoretical edge spread function (ESF) [see Fig. 3(b)], which could be calculated by integrating the 2D point spread function (PSF). In this way, the lateral resolution was quantified as 0.50 ± 0.05

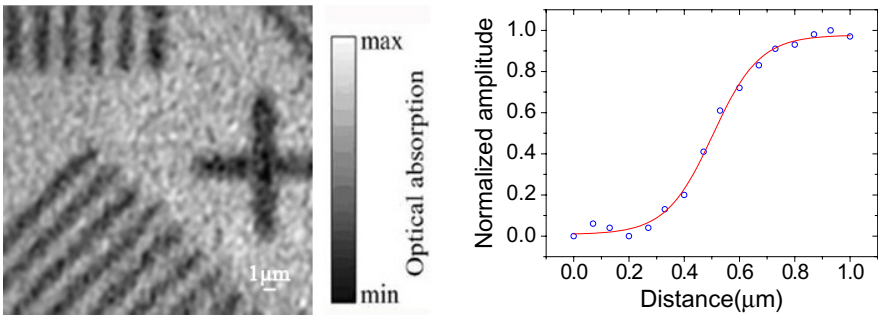

(a) (b)

Fig. 3. Lateral resolution of the OR-PAM system. (a) PAM image of the resolution test target (RTA-07). (b) By fitting the ESF given by the bars, the lateral resolution is quantified as $0.50 \pm 0.05\,\mu$m. The blue circles denote the experimental data, and the red curve is the theoretical fit.

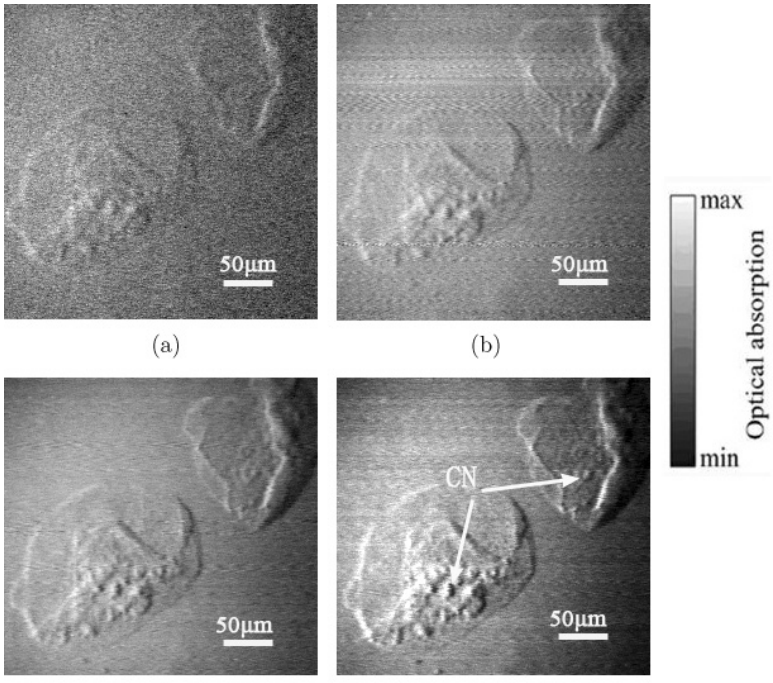

(a) (b) (c) (d)

Fig. 4. Comparison of OR-PAM images of oral epidermal cells acquired through simultaneous acquisition with different numbers of sensors. (a) Single-sensor PAM image, (b) two-sensor PAM image, (c) three-sensor PAM image and (d) four-sensor PAM image. CN: cell nucleus.

μm by fitting the data from 16 edges. Therefore, we claim that the OR-PAM has a lateral resolution of $\sim 500\,\text{nm}$, a value that represents the lateral resolution of the system and is very close to the theoretical value of $0.51\lambda/\text{NA} \approx 525\,nm$.

3.2. *Improvement by simultaneous multi-probe microscopy acquisition*

As previously mentioned, the amplitude of a PA signal depends on the absorption coefficient of the sample and on the illuminated light. Oral epidermal cells with weak optical absorption were utilized in the experiments to demonstrate the high sensitivity and SNR of the developed PAM (see Fig. 4). The image had a field of view of $320 \times 320\,\mu$m. Figure 4(a) shows the PAM image of two oral epidermal cells with one sensor. The number of sensors was gradually increased to four [see Figs. 4(b) to 4(d)]. The SNRs in Figs. 4(a) to 4(d) measure 17, 20, 22 and 23 dB, respectively. SNR was improved by 6 dB with the developed OR-PAM through simultaneous four-probe microscopy acquisition. Image contrast was enhanced accordingly; thus, the cell nuclei of the oral epidermal cells were observed clearly [see Fig. 4(d)].

4. Conclusion

A multi-probe label-free CW-mode OR-PAM was developed through simultaneous multi-probe microscopy acquisition technique. The lateral resolution of the test target was $\sim 500\,\text{nm}$. Imaging of oral epidermal cells with weak optical absorption indicates that the SNR of the four-sensor OR-PAM improved by 6 dB compared with that of the single-sensor OR-PAM. This result indicates that the technique can effectively enhance detection sensitivity and PAM image contrast. All these results demonstrate that the developed OR-PAM system can be applied in the detection of label-free cancer cells at the sub-cellular level, which is useful in intracellular photodynamic therapy and drug delivery research.

Acknowledgments

This work is supported by the National Natural Science Foundation of China (Grant No. 61178086), Science and Technology Program of Guangzhou, China (Grant No. 2012J4300138), Foundation for Distinguished Young Talents in South China Normal University, China. (Grant No. 2012KJ010).

References

1. S. Hu, B. Rao, K. Maslov, L. V. Wang, "Label-free photoacoustic ophthalmic angiography ", *Opt. Lett.* **35**(1), 54−56 (2010).
2. K. Maslov, H. F. Zhang, S. Hu, L. V. Wang, "Optical-resolution photoacoustic microscopy for in vivo imaging of single capillaries," *Opt. Lett.* **33**(9), 929−931 (2008).
3. C. Zhang, K. Maslov, L. V. Wan, "Subwavelength-resolution label-free photoacoustic microscopy of optical absorption in vivo," *Opt. Lett.* **35**(19), 3195−3197 (2010).
4. S. Yang, F. Ye, D. Xing, "Intracellular label-free gold nanorods imaging with photoacoustic microscopy," *Opt. Express* **20**(9), 10370−10375 (2012).
5. T. Zhou, B. Wu, D. Xing, "Bio-modified Fe_3O_4 core/Au shell nanoparticles for targeting and multimodal imaging of cancer cells," *J. Mater. Chem.* **22**, 470−477 (2012).
6. Z. Ji, Y. Fu, S. Yang, "Microwave-induced thermoacoustic imaging for early breast cancer detection," *J. Innov. Opt. Health Sci.* **6**(1), 1350001 (2013).
7. S. Hu, K. Maslov, L. V. Wang, "Second-generation optical-resolution photoacoustic microscopy with improved sensitivity and speed," *Opt. Lett.* **36**(7), 1134−1136 (2011).
8. L. V. Wang, S. Hu, "Photoacoustic tomography: In vivo imaging from organelles to organs," *Science* **335**(6075), 1458−1462 (2012).
9. S. Hu, K. Maslov, V. Tsytsarev, L. V. Wang, "Functional transcranial brain imaging by optical resolution photoacoustic microscopy," *J. Biomed. Opt.* **14**(4), 040503 (2009).
10. S. Hu, K. Maslov, L. V. Wang, "Noninvasive label-free imaging of microhemodynamics by optical-resolution photoacoustic microscopy," *Opt. Express* **17**(9), 7688−7693 (2009).
11. Z. Tan, Z. Tang, Y. Wu, Y. Liao, W. Dong, L. Guo, "Multimodal subcellular imaging with microcavity Photoacoustic transducer," *Opt. Express* **19**(3), 2426−2431 (2011).
12. T. Jetzfellner, V. Ntziachristos, "Performance of blind deconvolution in optoacoustic tomography," *J. Innov. Opt. Health Sci.* **4**(4), 385−393 (2011).
13. L. Silvestri, A. L. Allegra Mascaro, J. Lotti *et al.*, "Advanced optical techniques to explore brain structure and function," *J. Innov. Opt. Health Sci.* **6**(1), 1230002 (2012).

14. L. V. Wang, "Multiscale photoacoustic microscopy and computed tomography," *Nat. Photonics* **3**, 503−509 (2009).
15. L. Zeng, D. Xing, H. Gu, D. Yang, S. Yang, L. Xiang, "High antinoise photoacoustic tomography based on a modified filtered backprojection algorithm with combination wavelet," *Med. Phys.* **34**(2), 556−563 (2007).
16. W. Xia, D. Piras, J. V. Hespen, S. V. Veldhoven, C. Prins, T. VanLeeuwen, W. Steenbergen, S. Manohar, "An optimized ultrasound detector for photoacoustic breast tomography," *Med. Phys.* **40**, 032901 (2013).
17. A. Rosencwaig, A. J. Gersho, "Theory of the photoacoustic effect with solids," *J. Appl. Phys.* **47**(1), 64−69 (1976).
18. Laser Institute of America, American national standard for safe use of lasers ANSI Z136.1-2007, American National Standards Institute, Inc. (2007).